[6]Volker Heine, Phys. Rev. 138, A1689 (1965).
[7]J. Bardeen, L. N. Cooper, and J. R. Schrieffer, Phys. Rev. **106**, 162 (1957); Phys. Rev. **108**, 1175 (1957).
[8]David Pines, *Elementary Excitations in Solids* (Benjamin, New York, 1964), Chap. 3, pp. 96–98.
[9]J. Lindhard, K. Dan. Vidensk. Selsk. Mat.-Fys. Medd. **28**, 8 (1954).
[10]D. Pines, in Ref. 8, Chap. 3, p.158.
[11]P. B. Allen (private communication).
[12]W. L. Mcmillan, Phys. Rev. **167**, 331 (1968).
[13]D. Pines, in Ref. 8, Chap. 4, pp. 173 and 200.
[14]H. R. Phillip and H. Ehrenreich, Phys. Rev. **129**, 1550 (1963).
[15]D. J. Scalapino, Y. Wada, and J. C. Swihart, Phys. Rev. Lett. **14**, 102 (1965).
[16]C. R. Leavens and J. P. Carbotte, Can. J. Phys. **49**, 724 (1971).
[17]P. Hertel, Z. Phys. **248**, 272 (1971).
[18]V. L. Ginzburg, ZhETF Pis. Red. **14**, 572 (1971) [Sov. Phys.-JETP Lett. **14**, 396 (1971)].

PHYSICAL REVIEW B VOLUME 7, NUMBER 3 1 FEBRUARY 1973

Electron Spin Resonance and Superconductivity in $Gd_xLa_{1-x}Al_2$ Intermetallic Compounds*

D. Davidov, A. Chelkowski,† C. Rettori,‡ and R. Orbach
Department of Physics, University of California, Los Angeles, California 90024

and

M. B. Maple§
Department of Physics, University of California, San Diego, California 92037

(Received 7 August 1972)

Electron-spin-resonance measurements of Gd in $LaAl_2$ exhibit appreciable change of the g value and linewidth upon alloying with other nonmagnetic impurities. This indicates the existence of a "bottleneck" effect—the relaxation rate for the conduction electrons to the Gd ions δ_{ei} exceeds that to the lattice δ_{eL}. We are able to shift the g value from $g = 1.988 \pm 0.003$ to $g = 2.11 \pm 0.01$, opening the bottleneck completely. The intermetallic compounds $GdLa_{1-x}Al_2$ are Abrikosov–Gorkov superconductors in the dilute limit. Measurements of the transition temperature and the upper critical field depend upon δ_{ei} directly and δ_{eL} indirectly. We are thus able to obtain parameters which determine superconducting critical-field and temperature behavior from magnetic resonance experiments.

I. INTRODUCTION

Previous electron-spin-resonance measurements of Gd in concentrated $GdAl_2$ indicate a negative g shift[1,2] which has been interpreted in terms of a negative exchange interaction between the Gd $4f$ and the conduction electrons. Assuming a rigid-band model, one would expect that substitution of La in place of Gd would not appreciably change the conduction-band structure, and thus the g shift. It was surprising, therefore, that the g shift of dilute (in retrospect, partially unbottlenecked) $LaAl_2$: Gd was found to be positive.[3] The purpose of this paper is to present new experimental data on this system. We shall demonstrate the existence of a bottleneck in the exchange relaxation mechanism. By introducing other (nonmagnetic) impurities we are able to shift the g value from $g = 1.988 \pm 0.003$ (a small negative shift) to $g = 2.11 \pm 0.01$ (a large positive shift), opening the bottleneck completely. We shall show that our experimental data, as well as the electron-paramagnetic-resonance (EPR) results of others[1–3] for the dilute and the magnetically dense $Gd_xLa_{1-x}Al_2$ system, are consistent with a two-band model. This removes the experimental "discrepancy" between the EPR results for the magnetically concentrated and dilute alloys.

A condition for a bottleneck in the electron spin resonance of dilute magnetic alloys is that the conduction electrons's relaxation rate to the paramagnetic ions δ_{ei} exceeds that to the lattice δ_{eL}. The former can be changed by changing the concentration of the paramagnetic impurities. The latter is very sensitive to any nonmagnetic "dirt," and therefore to the hard-to-control method of preparation. An advantage of using $LaAl_2$ as a nonmagnetic host is its superconductivity. The intermetallic compounds $Gd_xLa_{1-x}Al_2$ (in the dilute limit) are Abrikosov–Gorkov superconductors,[4] so that T_c measurements provide information about the concentration and exchange scattering rate of the magnetic impurities, while H_{c2} measurements (upper critical field) give in addition information about the potential scattering rate of any nonmagnetic impurities. This enables us to control and measure δ_{ei} directly and δ_{eL} indirectly, independent of the EPR results. The correlation between these two techniques enables one to check the Hasegawa[5] model in a critical manner.

We shall present sample preparation and analysis in Sec. II, the EPR results in Sec. III, the superconducting behavior in Sec. IV, the interpretation in Sec. V, and the summary of our results in Sec. VI. We shall demonstrate that EPR can

enable one to obtain those parameters which determine changes in the transition temperature and the upper critical field of type-II superconductors.

II. SAMPLE PREPARATION AND ANALYSIS

The $Gd_xLa_{1-x}Al_2$ samples were prepared in an arc furnace in an argon atmosphere. We used arc furnaces at both the University of California, Los Angeles (UCLA) and the University of California, San Diego (UCSD). All the samples were melted many times, beginning with a master sample and step-by-step dilution. The superconductivity measurements were performed on arc-melted balls (approximately 3 mm diam). The EPR was performed on powder samples prepared from the balls. Different EPR and correlated superconducting results were obtained for samples prepared in the two different arc furnaces, even at the same Gd concentration. X-ray analyses indicate that all samples were of the $LaAl_2$ crystal structure. Figure 1 exhibits the EPR results for two series of samples prepared in the different arc furnaces. The closed circles represent samples prepared at UCSD; the open circles the same samples remelted at UCLA. The differences are remarkable. To our knowledge, the only difference between the two furnaces was the purity of the argon. In both of them, ultrahigh-purity grade argon from Matheson was used. However, at UCLA the argon was further purified by passing it through cold traps both before and after bubbling it through a eutectic Na-K alloy ($Na_{0.33}K_{0.67}$) to remove the last trace of water and oxygen.

Superconductivity measurements provide further information about the quality of the samples. (i) The superconducting transition temperature T_c provides us with a measurement of the concentration of the magnetic impurities in the samples (Gd). (ii) The width of the superconducting transition, δT_c, gives a measure of the homogeneity of the Gd-impurity distribution in the samples. We obtained a correlation between this width and the residual width of the EPR lines. (iii) Measurements of the upper critical field $H_{c2}(T)$ gives information about the nonmagnetic "dirt" in the samples (or the residual resistivity due to the nonmagnetic impurities).

We found that samples prepared at UCSD, and afterwards remelted at UCLA, exhibited roughly the same T_c, while $H_{c2}(T)$ and δT_c changed appreciably. We shall demonstrate in Sec. V that the differences in $H_{c2}(T)$ correlate with differences in the EPR properties.

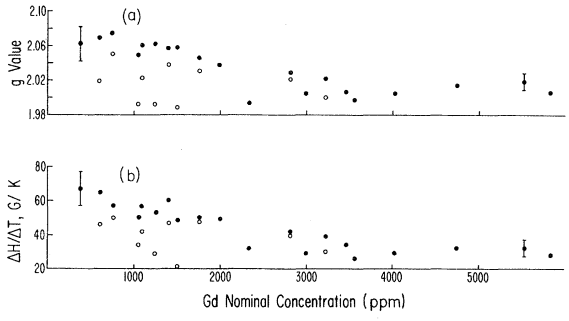

FIG. 1. (a) Effective g value of Gd in $Gd_xLa_{1-x}Al_2$ as a function of Gd concentration (nominal at 1.4 K). (b) Thermal broadening $\Delta H/\Delta T$ as a function of Gd concentration for the same $Gd_xLa_{1-x}Al_2$ samples exhibited in (a). Closed circles represent samples prepared at UCSD; open circles represent the same samples remelted at UCLA.

III. EPR RESULTS

The EPR was performed primarily at X band, and as a function of temperature in the liquid-helium range ($1.4 \leq T \leq 4.2$ K). A few measurements were also performed at Q band and at high temperatures (13–20 K). However, the large linewidth at Q band and high temperatures increased the uncertainty in the measured value of the g shift, and there were no truly conclusive results from these measurements. We found that the g shift and $\Delta H/\Delta T$ (the temperature slope of the linewidth) were extremely sensitive to the method of sample preparation as explained above (see Fig. 1).

Figure 2 exhibits the linewidth vs temperature for some of the $Gd_xLa_{1-x}Al_2$ samples prepared at UCSD. For comparison, we also present the linewidth of one sample after remelting at UCLA. It is clearly seen that both the residual width and the slope of the linewidth vs temperature are appreciably smaller in the latter sample as compared to the former samples.

The actual EPR absorption spectra, observed for two $Gd_xLa_{1-x}Al_2$ samples, are presented in Fig. 3. The absorption associated with the superconducting state below the critical field, as well as the EPR signal of the Gd, is clearly seen. Below the concentration of 300-ppm Gd the critical field is large enough to overlap with the field for the resonance of the Gd, and no satisfactory EPR measurements could be obtained. The EPR results can be summarized as follows.

(i) The g value and linewidth ΔH change appreciable from one sample to another (Fig. 1). Any increase in the slope of the linewidth is always associated with an appropriate increase in the effective g value. This indicates the presence of a magnetic-resonance bottleneck.[5]

(ii) The lowest value obtained for g is 1.988 ± 0.003. This value was confirmed at the Q band. The value obtained previously for $GdAl_2$ was 1.982 ± 0.005. The smallest observed value of $\Delta H/\Delta T$ was 20 G/K.

(iii) Substitution of $ThAl_2$ in place of $LaAl_2$ in

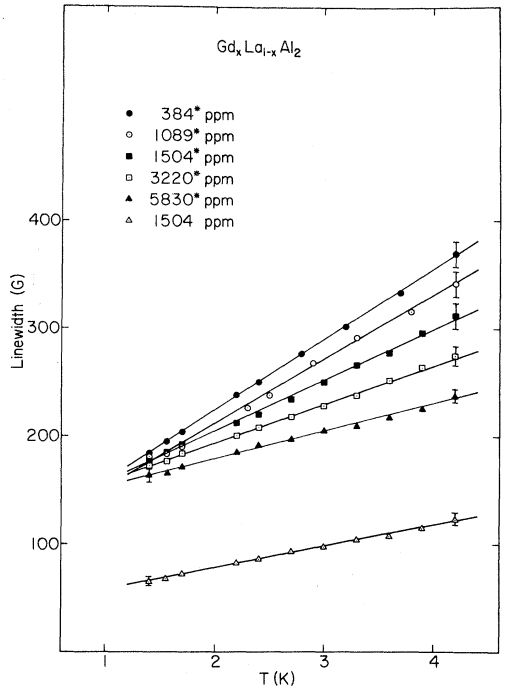

FIG. 2. Linewidth vs temperature of some $Gd_xLa_{1-x}Al_2$ samples prepared at UCSD (starred in the figure). For comparison the linewidth of one sample (1440 ppm) remelted at UCLA is shown (not starred).

$Gd_xLa_{1-x}Al_2$ increases both Δg and $\Delta H/\Delta T$ (see Figs. 4–6). The maximum value of Δg and $\Delta H/\Delta T$ is 0.11 ± 0.01 [6] and 70 G/K, respectively. These values are independent of further increases in Th concentration (Fig. 6), and are identified as the fully unbottlenecked g shift and linewidth.

(iv) The g value was slightly temperature dependent, increasing by 0.01 ± 0.01 in the high-temperature limit. This effect, as well as low- and high-field measurements, indicates that the dynamic effect,[7,8] though small at high temperature (4.2 K), cannot be completely neglected here. The increase in Δg was always associated with an increase in the A/B ratio, where A and B are the heights of the low- and high-field peaks in the derivative absorption spectrum referred to the base line, respectively (see Fig. 3 for two examples of resonance line shapes). The apparent g shift associated with this increase is in the same direction as the dynamic effect, and is of nearly the same magnitude. As a result we are unable to determine if the dynamic effect is present. If it is, it is small. The difficulty of determining the A/B ratio at high temperatures leads to the relatively large error bars for the g value in that region.

IV. SUPERCONDUCTIVITY

The upper critical field vs temperature was measured using a mutual-induction technique. All the measurements presented in this paper were performed at 20-kc frequency. The change in the voltage induced in the secondary coil (due to change in the susceptibility as a result of the superconducting transition) is plotted in Fig. 7. The upper critical field was determined by extrapolation as shown in Fig. 7. We shall denote the extrapolated values by H_{c2} throughout the paper.

There is some disadvantage in using the mutual-induction technique for H_{c2} measurements rather than the specific heat. The reason is that the former is also very sensitive to surface superconductivity (H_{c3}). Indeed, a slight frequency dependence was found in our measurement of H_{c2}. The broad transition at the high critical field makes the exact determination and separation of H_{c2} and H_{c3} difficult, leading (according to our estimate) to a 15% error in H_{c2}. However, in the present work we are interested in the relative change of H_{c2} (compared to "pure" $LaAl_2$). We found these relative changes to be much larger than the error in H_{c2} due to the

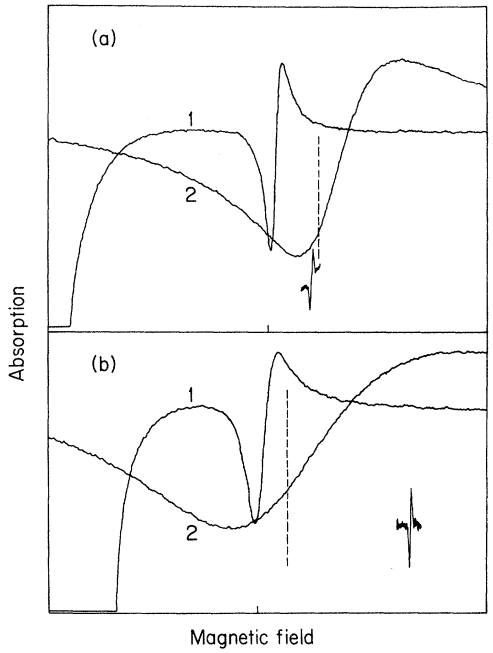

FIG. 3. Spectra observed for (a) the 1050-ppm Gd in $LaAl_2$ sample at 1.4 K and (b) the same sample but after introducing 1.5-at.% $ThAl_2$ in place of $LaAl_2$. The central field is 2850 G. The spectra denoted by (1) in both (a) and (b) were observed by sweeping the magnetic field over a range of 5000 G; the sweep range for the spectra denoted by (2), as well as for the DPPH marker, is 500 G. The signal at the left-hand side of the figure is due to superconducting absorption below the critical magnetic field; that in the center of the figure [in both (1) and (2)] is the EPR of the Gd. The vertical dashed line is the field for resonance of the Gd for a 500-G sweep. It is clearly seen that the large g shift in (b) is associated with an increase of the upper critical field.

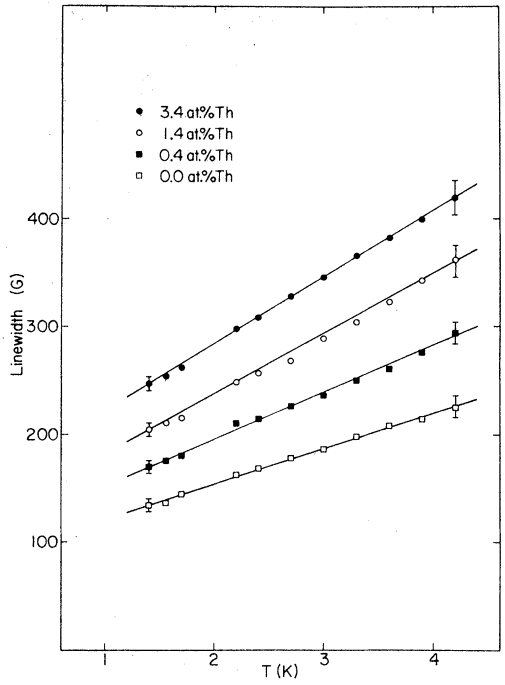

FIG. 4. EPR linewidth of Gd (2330 ppm) in $Th_xLa_{1-x-0.00233}Al_2$ as a function of temperature. The thorium concentration is denoted on the figure. The samples were prepared at UCLA. The effect of substituting Th in place of LA is to increase both $\Delta H/\Delta T$ and the residual width.

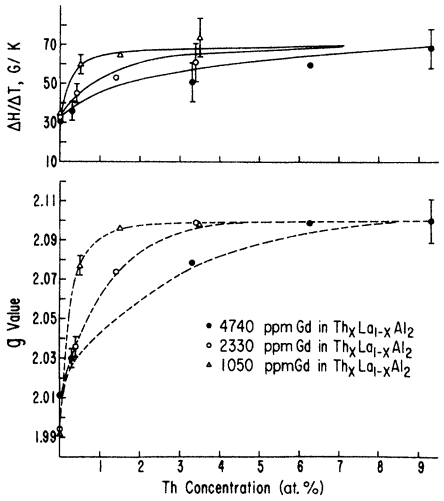

FIG. 6. Effect of substituting Th in place of La on the linewidth of Gd and the g value. The solid lines are the theoretical linewidths obtained by using Eq. (2b) and the values of δ^s_{eL} extracted from the g-value–vs–concentration plot.

width of the transition. Thus, although the error in the absolute value of H_{c2} (as determined in Fig. 7) may be large, we have confidence in the relative values. The samples were measured in the form of small balls or chips (almost no difference in results was obtained between the two forms). The coil axis was parallel or perpendicular to the external field (again, with almost no detectable difference). The superconducting transition temperature was determined by direct measurement and by extrapolating $H_{c2}(T)$ to $H_{c2}(T_c)=0$. The values of $H_{c2}(T)$ are in agreement (i.e., proportional) with those determined by microwave absorption (see Fig. 3). It should be stressed that the extrapolations (in Fig. 4) have been done in a consistent way for all the samples measured in order to diminish relative

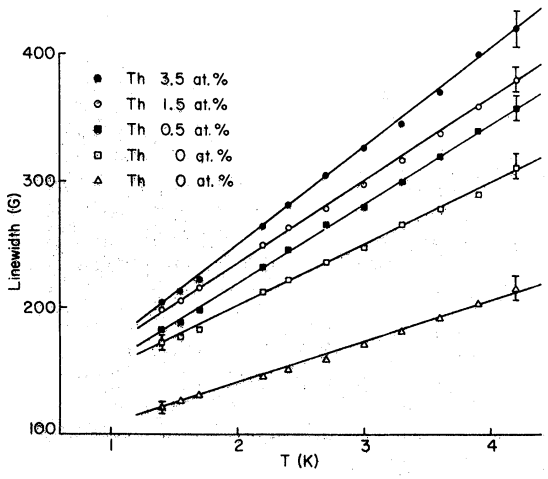

FIG. 5. EPR linewidth of Gd (1050 ppm relative to La) in $Th_xLa_{(1-x-0.00105)}Al_2$ as a function of temperature. The samples were prepared at UCSD. One sample was remelted at UCLA.

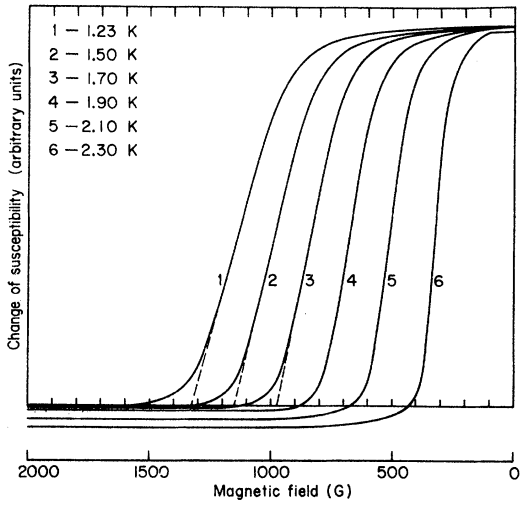

FIG. 7. Change in susceptibility of $La_{1-x}Gd_xAl_2$ vs magnetic field at various temperatures. The critical fields are determined by extrapolation (dashed lines). The Gd concentration was 1400 ppm ($x=0.0014$).

errors in H_{c2}.

Figures 8 and 9 exhibit the effect of nonmagnetic impurities (Th) on the upper critical field. It is clearly seen that while H_{c2} changes appreciably (probably due to changes in the residual resistivity), T_c hardly varies. Figures 10 and 11 fit our experimental data to the theory of Abrikosov and Gorkov.

In the dirty limit,[9] the value of H_{c2} as a function of T in the presence of two depairing mechanisms, (i) externally applied field and (ii) magnetic impurities, is given by[10,11]

$$\ln(T_c/T_{c0}) + \psi(\tfrac{1}{2}+\rho) - \psi(\tfrac{1}{2}) = 0 \quad \text{and} \quad (1)$$

$$\rho = 0.140\,\frac{T_{c0}}{T_c}\left(\frac{\tau_{tr}H_{c2}(T)}{\tau_{tr\,0}H_{c2\,0}(0)} + \frac{n}{n_{cr}}\right),$$

where $\tau_{tr\,0}$ and $H_{c2\,0}$ are the transport collision time and the upper critical field for pure $LaAl_2$, respectively, and $\psi(x)$ is the digamma function, defined by $\psi(x) = d(\ln x!)/dx$. The quantities n and n_{cr} are the concentration and the critical concentration of the Gd magnetic impurities, respectively. For $Gd_xLa_{1-x}Al_2$, $n_{cr} = 0.560$ at.%. The normalized pair breaking parameter, in the present case

$$\frac{\tau_{tr}H_{c2}(T)}{\tau_{tr\,0}H_{c2\,0}(0)} + \frac{n}{n_{cr}},$$

as a function of the reduced temperature T/T_{c0} is tabulated in Ref. 12.

For pure $LaAl_2$ (i.e., Gd absent), $n = 0$. Therefore, any variation in H_{c2} from one sample to another may be attributed to a change in $\tau_{tr}/\tau_{tr\,0}$. Different $LaAl_2$ samples exhibit different H_{c2} (see Table I). We choose the value of $\tau_{tr}/\tau_{tr\,0}$ to be equal to 1 for the $LaAl_2$ sample with the lowest value of $H_{c2}(T)$. This is possible according to Eqs. (1) if and only if the upper critical field at 0 K for this particular sample is identical with $H_{c2\,0}(0)$. We therefore find $H_{c2\,0}(0) = 2400$ G. The values of $\tau_{tr}/\tau_{tr\,0}$ for all the other samples are normalized with respect to this particular $LaAl_2$ sample.

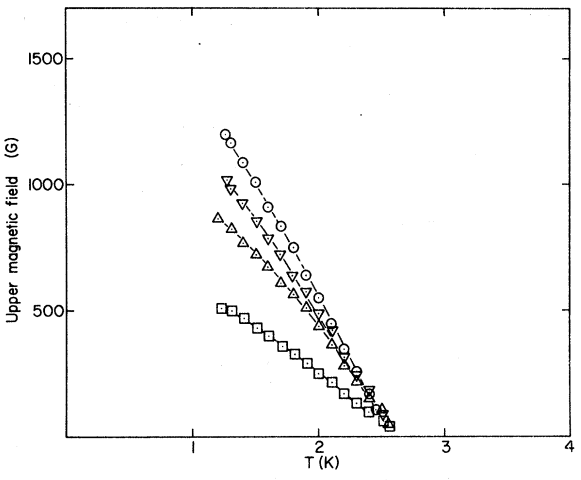

FIG. 8. Upper critical field H_{c2} as a function of temperature for various $Gd_xTh_yLa_{1-x-y}Al_2$ samples. The value of x is always $x = 0.001\,050$ (1050 ppm). The values of y are as follows: The circles represent samples with $y = 0.035$; the inverted triangle with $y = 0.015$; the triangles with $y = 0.005$ (5000-ppm Th); and the squares with $y = 0$. The effect of substituting Th in place of La is to increase H_{c2}. The samples were prepared at UCSD.

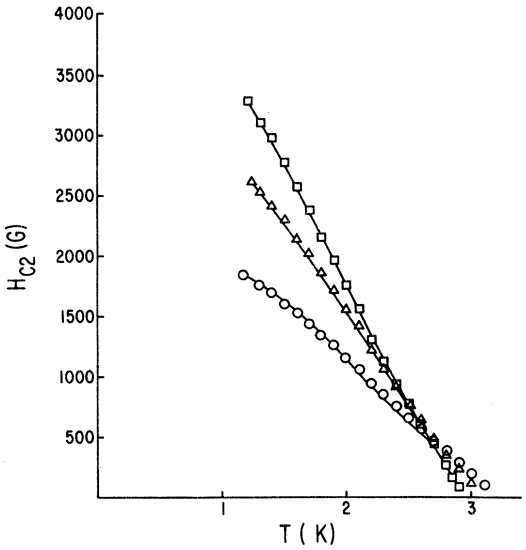

FIG. 9. Upper critical field as a function of temperature for various $Th_xLa_{1-x}Al_2$ samples. The Th concentration in the various samples is as follows: the squares represent samples with $x = 0.042$; the triangles represent samples with $x = 0.023$; and the circles represent samples with $x = 0$.

For samples which contain Gd ions ($n \neq 0$) the estimation of $\tau_{tr}/\tau_{tr\,0}$ is obtained in two steps. First we subtract the effect of Gd impurities on H_{c2} using the method described by Parks.[13] This is possible because T_c and n/n_{cr} are known. Then we fit $H_{c2}(T)$ vs T to the Abrikosov–Gorkov result (Figs. 9 and 10) to extract $\tau_{tr}/\tau_{tr\,0}$ (again, normalized to pure $LaAl_2$) for the various samples. We assume that substitution of Gd for La does not change τ_{tr} appreciably. Such an assumption has been made previously for $(Gd_xLa_{1-x})_3Al$.[10] Thus, any change in τ_{tr} is assumed to originate with nonmagnetic impurities.

Table I exhibits the values of $\tau_{tr\,0}/\tau_{tr}$, as well as τ_c and $H_{c2}(0)$, for various $Gd_xLa_{1-x}Al_2$ samples (see Fig. 1). The value of T_c directly yields the concentration of the magnetic impurities (gadolinium), and we denote this value in Table I by the symbol n_{AG}. For comparison, we have also given the values of Δg and $\Delta H/\Delta T$ found by EPR on the same

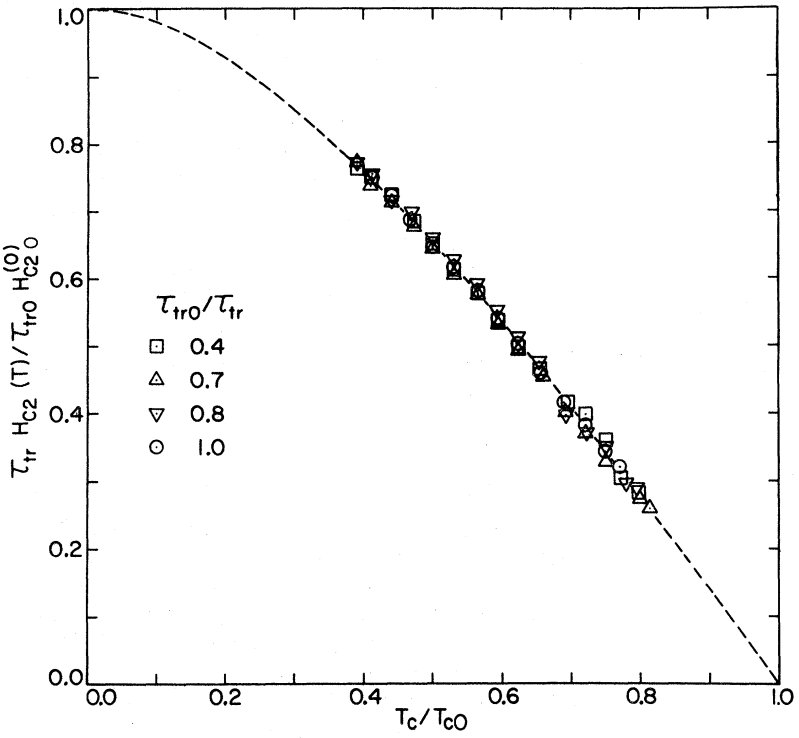

FIG. 10. Fitting of the results in Fig. 8 to Abrikosov–Gorkov theory (dashed line). The squares, triangles, and circles represent samples with different Th concentrations. The values of τ_{tr0}/τ_{tr} for the various samples are listed in the figure.

samples. The remarkable "proportionality" between Δg (and $\Delta H/\Delta T$) and $1/\tau_{tr}$ is clearly seen. Whenever the former two quantities are large, a larger value results for the latter. This relationship will be examined quantitatively below.

V. INTERPRETATION

The variation of Δg from a negative to positive values, as well as the fact that $\Delta H/\Delta T$ has relatively large magnitudes (at least 20 G/K), even for samples which exhibit zero g shift, indicates that a simple one-band model (free-electron picture) is inapplicable here. We therefore propose a two-band model of the following character. (i) The exchange interaction J_{f-s} between the Gd $4f$ electrons and the s-band conduction electrons is positive. The s band relaxes weakly to the lattice and is therefore bottlenecked. (ii) The exchange interaction J_{f-d} between the Gd $4f$ electrons and the d-band conduction electrons is negative.[14] The d band relaxes rapidly to the lattice and is therefore unbottlenecked.

These assumptions lead to the following equations for the linewidth and g shift[5,8]:

$$\Delta g = \Delta g_d + \Delta g_s \left(\frac{x^2}{(1+x)^2+y^2} \right) , \tag{2a}$$

$$\Delta H = \frac{\pi k_B T}{g\mu_B} \left[(\Delta g_d)^2 F_d K_d(\alpha_d) + (\Delta g_s)^2 K_s(\alpha_s) \left(\frac{x(1+x)+y^2 x}{(1+x)^2+y^2} \right) \right] , \tag{2b}$$

$$\Delta g_d = J_{f-d}\, \eta_d\, [1/(1-\alpha_d)] , \tag{2c}$$

$$\Delta g_s = J_{f-s}\, \eta_s\, [1/(1-\alpha_s)] , \tag{2d}$$

where Δg_d and Δg_s are the g shifts associated with the d and s bands, respectively. F_d is a reduction factor associated with the degeneracy of the d levels at the Fermi energy, and x and y equal $\delta_{eL}^s/\delta_{ei}^s$ and $\gamma\lambda\chi_t H/\delta_{ei}^s$, respectively, in an obvious notation. The quantities α_s, α_d, $K_s(\alpha_s)$, and $K_d(\alpha_d)$ are enhancement factors caused by exchange enhancement of the conduction-electron susceptibility. They are defined and tabulated in Ref. 15. Equations (2) were derived in analogy with previous Knight-shift and relaxation calculations for nuclei in cubic symmetry. According to these calculations, there are no interference terms between s and d relaxation mechanisms in cubic symmetry, even in the presence of s-d mixing.[16]

The maximum negative shift observed in our experiments is $\Delta g = -0.01 \pm 0.004$. We suggest that this shift corresponds to a situation in which the magnetic-resonance bottleneck associated with the s band is complete, but no bottleneck is present for the d band. The negative g shift is consistent with that found in the magnetically dense compound $GdAl_2$. We assume, therefore, that $\Delta g_d = -0.01$. The value of Δg_s must therefore equal $+0.12 \pm 0.01$.

With this assumption, Eq. (2a) agrees with experiment. In the bottleneck regime ($\delta_{ei}^s > \delta_{eL}^s$), the g shift is negative; in the unbottlenecked regime ($\delta_{eL}^s \gg \delta_{ei}^s$), the total g shift is $\Delta g = 0.11 \pm 0.01$.

Equation (2b) also agrees with experiment if we take $K_s(\alpha_s) = 0.28$. This value is in disagreement with that obtained from Ref. 15 using a value for α_s derived from susceptibility enhancement (see below).

Specific-heat measurements on $LaAl_2$, YAl_2, and $LuAl_2$[17] indicate that the value of γ for $LaAl_2$ equals 3.65 mJ/g atom K^2, to be compared with the value of γ found for YAl_2 or $LuAl_2$, equal to 1.90 mJ/g atom K^2. After subtracting the electron-phonon mass-enhancement contribution to the specific heat using the formula of McMillan,[18] we find a "bare" density of states for $LaAl_2$ equal to $\eta_\gamma = 0.47$ states/eV atom spin. The density of states for YAl_2 or $LuAl_2$ is 0.35 states/eV atom spin, smaller than in $LaAl_2$, indicating substantial narrow-band contributions to γ in $LaAl_2$. Additional evidence for the existence of narrow d bands in $LaAl_2$ is provided by recent resistivity measurements.[19,20] A negative curvature above 150 K in the electrical resistivity of $LaAl_2$ is found, and attributed to the scattering of s electrons into the d states, as proposed by Mott.[21] The curvature in the resistivity of YAl_2 is much less pronounced, indicating that narrow-band (d-band) contributions are small.

We assume therefore that the following separation holds:

$\eta_s = 0.35$ states/eV atom spin,

$\eta_d = 0.12$ states/eV atom spin.

The susceptibilities of $LaAl_2$[19,22] and YAl_2[22] (corrected for core and diamagnetic contributions) are 2.25×10^{-4} emu/mole and 4.83×10^{-6} emu/cm^3, respectively. The densities of states associated with these susceptibilities η_χ are much larger than those associated with the specific heat η_γ, indicating strong electron-electron exchange enhancement. We estimate η_χ/η_γ to equal 2.3 and 2.4 (these values were calculated neglecting the electron-phonon mass enhancement) for $LaAl_2$ and YAl_2, respectively. Because we assume that the d contribution in YAl_2 is negligible, we can take the above ratio for YAl_2 to estimate α_s. We find $\alpha_s = 0.56$. The value of $K_s(\alpha_s)$ associated with this value of α_s, according to Shaw and Warren,[15] is $K(\alpha) = 0.35$, larger than the value $[K_s(\alpha_s) = 0.28]$ necessary to fit our g shift and linewidth. It should be stressed that the value of $K(\alpha)$ should be very sensitive to the $\vec{q}$ dependence of the electron-electron interaction, and may be completely different for $LaAl_2$ than for other materials, for the same α. The d contribution to the linewidth is estimated to be less than 5 G/K, whatever value of F_d we use. This is less than the experimental error, and will be neglected. The experimental value of $\Delta H/\Delta T$ in the unbottlenecked regime yields a value for the relaxation of the paramagnetic ions to the s band of $\delta^s_{ie} = 1.4\times10^9 T\ \mathrm{sec}^{-1}$. The value of δ^s_{ei} is found from the detailed balance condition $\delta^s_{ei} = (\chi_i/\chi^s_e)\delta^s_{ie}$.[23] Knowledge of δ^s_{ei} enables the extraction of δ^s_{eL} for the various samples, using Eq. (2a). The solid lines in Fig. 6 are the theoretical linewidths [ac-

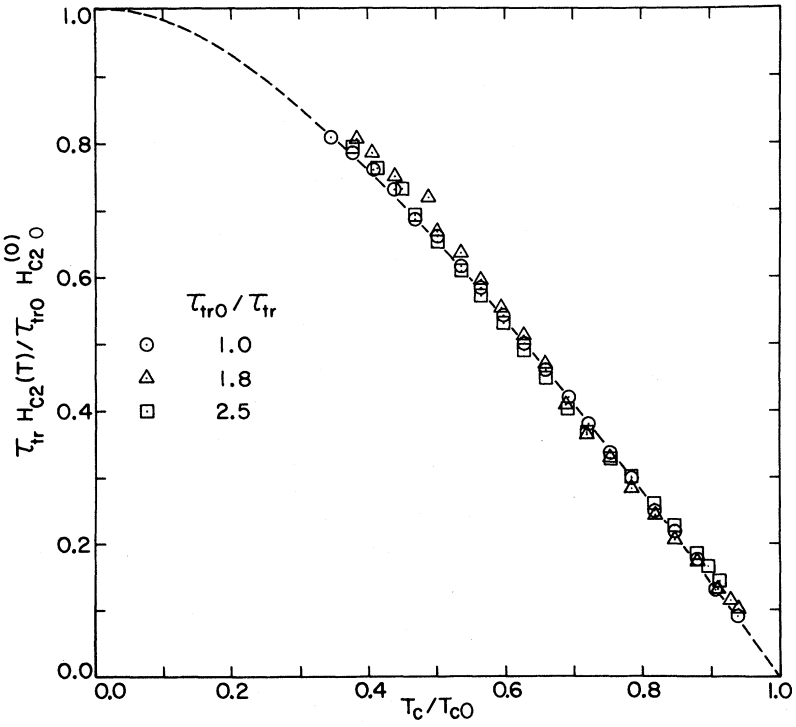

FIG. 11. Fitting of the results in Fig. 9 to Abrikosov–Gorkov theory (dashed line). The circles, triangles, and squares represent samples with different Th concentrations (see Fig. 9). The values of τ_{tr0}/τ_{tr} for the various samples are shown on the figure.

TABLE I. Comparison between superconductivity and EPR results for various $Gd_xLa_{1-x}Al_2$ samples. T_c is the superconducting transition temperature determined by extrapolating $H_{c2}(T)$ to $H_{c2}(T_c)=0$. The error bars in T_c are ± 0.06 K for low Gd concentration (less than 1500 ppm) and ± 0.1 K for high Gd concentration. T_c^{**} is the superconducting transition temperature in the absence of the magnetic field; n_{AG} is the Abrikosov–Gorkov concentration of the Gd ion as determined from Fig. 7, knowing T_c and $n_{cr}=0.560$ at.%. The error limits for n_{AG} are determined from the error limits for T_c (and n_{cr}). The ratio $\tau_{tr\,0}/\tau_{tr}$ was obtained by fitting $H_{c2}(T)$ vs T to the Abrikosov-Gorkov theory and normalized relative to $\tau_{tr\,0}$ of pure $LaAl_2$ (see text).

Nominal Gd conc. n (ppm)	Superconductivity T_c	T_c^{**}	n_{AG} (ppm)	H_{c2} (G) $T=1.4$ K	$\tau_{tr\,0}/\tau_{tr}$	H_{c2} (G) $T=0$ K	EPR g	$\Delta H/\Delta T$ (G/K)
0[a]	3.20	3.17	0	1700	1	2300	•••	•••
0[a]	3.20	3.17	0	2410	1.4 ± 0.1	3200	•••	•••
609[b]	2.86	2.81	840	820	0.6 ± 0.1	1150	2.019	46 ± 5
609[a]	2.92	2.90	700	1260	1.0 ± 0.1	1830	2.069	65 ± 10
754[b]	2.88	2.79	795	1100	0.8 ± 0.1	1640	2.050	50 ± 5
754[a]	2.88	2.82	795	1450	1.1 ± 0.1	2200	2.075	57 ± 10
1050[b]	2.65	2.54	1340	470	0.4 ± 1	720	1.992	34 ± 5
1050[a]	2.76	2.70	1060	1110	0.9 ± 1	1700	2.048	50 ± 5
1089[b]	2.80	2.67	930	870	0.7 ± 0.1	1280	2.022	43 ± 5
1239[b]	2.66	2.59	1320	590	0.5 ± 0.1	880	1.992	29 ± 5
1239[a]	2.72	2.64	1180	1290	1.2 ± 1	2000	2.062	53 ± 10
1400[b]	2.64	2.58	1370	995	0.9 ± 0.1	1580	2.038	46 ± 5
1400[a]	2.75	2.65	1100	1240	1.0 ± 0.1	1830	2.057	60 ± 10
1504[b]	2.48	2.35	1790	460	0.5 ± 0.1	770	1.988	20 ± 3
1504[a]	2.57	2.53	1510	1170	1.1 ± 0.1	1880	2.058	48 ± 5
1750[b]	2.44	2.39	1810	760	0.8 ± 0.1	1280	2.030	47 ± 5
1750[a]	2.58	2.47	1510	1000	0.9 ± 0.1	1560	2.046	49 ± 5
1990[a]	2.43	2.34	1865	1110	1.2 ± 0.1	1940	2.037	49 ± 5
2330[a]	2.24	2.20	2390	345	0.5 ± 0.1	680	1.993	32 ± 5
2810[b]	2.10	1.99	2590	610	1.0 ± 0.1	1240	2.021	37 ± 5
2810[a]	2.11	2.05	2590	670	1.1 ± 0.1	1390	2.029	41 ± 5
3460[b]	1.88	1.695	3060	380	1.0 ± 0.1	1000	2.023	40 ± 5
3550[a]	1.77	1.6	3300	140	0.5 ± 0.1	450	1.996	26 ± 3
4020[a]	1.52	1.37	3790	65	0.7 ± 0.1	510	2.004	29 ± 5

[a]UCSD samples. [b]Remelted at UCLA as described in text.

cording to Eq. 2(b)] using the value $K_s(\alpha_s)=0.28$, as well as the values for δ_{ei}^s and δ_{eL}^s quoted above. The agreement is satisfactory.

Finally, the extraordinary correlation between EPR measurements and superconductivity should be noted. The EPR analysis yields values for δ_{eL}^s, the spin-flip relaxation rate of the s-band conduction electrons to the lattice. H_{c2} measurements yield values for $1/\tau_{tr}$, the collision relaxation rate of the conduction electrons, assumed to be primarily s band insofar as the superconductivity is concerned. In the presence of nonmagnetic impurities, one expects these two quantities to be proportional. Indeed, when we extract values of δ_{eL}^s and $1/\tau_{tr}$ upon the addition of $ThAl_2$ into $LaAl_2$, we find a remarkable correlation (see Fig. 12). The solid line in Fig. 12 is the relation

$$\delta_{eL}^s - \delta_{eL}^{(0)} = 14\times10^{11}\,\tau_{tr\,0}\,[(1/\tau_{tr}) - (1/\tau_{tr}^{(0)})], \quad (3)$$

where $\delta_{eL}^{(0)}$ and $\tau_{tr}^{(0)}$ are the spin-lattice relaxation time and the collision relaxation time in the starting (Gd-doped) samples (i.e., before adding the $ThAl_2$). One can now use the resistivity data[19,20] to evaluate $\tau_{tr\,0}$. One finds the coefficient of the square bracket above to equal (approximately) 5×10^{-2}. This implies that the spin-flip scattering rate of the nonmagnetic impurities is two orders of magnitude smaller than the potential or transport scattering rate. This ratio varies as $(\lambda_{eff}/\Delta)^2[p^2/(1+p^2)]$, where λ_{eff} is the exchange enhanced spin-orbit coupling of the impurity state, Δ its width; and the mixing parameter $p=\Delta/(E_F-E)$, where E is the impurity-state energy.[24] Impurity s states do not contribute to spin flip, but

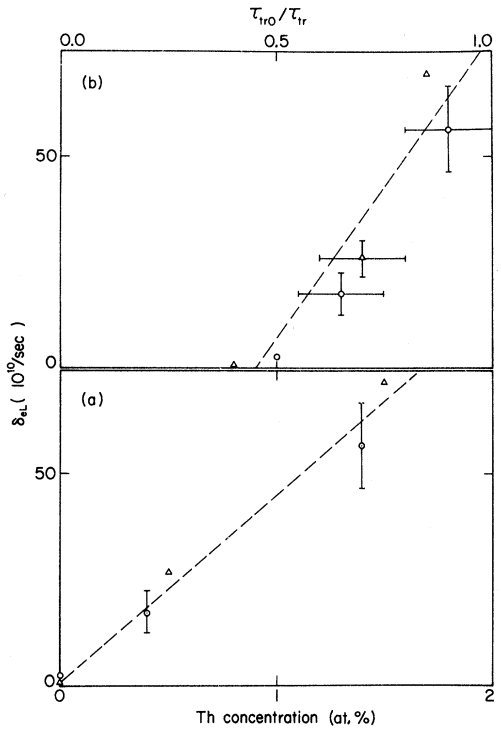

FIG. 12. (a) Value of δ^s_{eL} (extracted from the g shift of $Gd_xTh_yLa_{1-x-y}Al_2$) as a function of Th concentration. The triangles represent samples with $x = 0.001050$ (1050-ppm Gd); the circles represent samples with $x = 0.002330$ (2330-ppm Gd). (b) A plot of (3) using the same values for δ^s_{eL} as in (a). For the scale of this figure, $\delta^{(0)}_{eL}$ is not visible, so that the shift of the linear relationship between δ^s_{eL} and $\tau_{tr\,0}/\tau_{tr}$ is due to the "residual" (before the addition of Th) $\tau_{tr\,0}/\tau_{tr}{}^{(0)}$. $\tau_{tr\,0}/\tau_{tr}$ was extracted by fitting H_{c2} vs T to the Abrikosov–Gorkov theory.

do contribute to transport scattering. Reasonable values for λ_{eff}, Δ, and p give agreement with the measured coefficient.

Using the value of α_s and η_s, as well as the experimental g shift, we can estimate the exchange interaction J_{f-s}. We find $J_{f-s} = +0.13 \pm 0.01$ eV. Likewise, from the analogous quantities for the d band, we find $J_{f-d}/(1-\alpha_d) = -0.071$ eV. Assuming $\alpha_d = 0.5$, $J_{f-d} = -0.035$ eV. The value of the exchange interaction estimated from the initial decrease of T_c upon alloying with Gd ($\Delta T_c/\Delta c = 3.6$ K/at.% rare earth) is 0.1 ± 0.01 eV, leading to some degree of support for the position that the superconductivity originates primarily with s electrons in $LaAl_2$.[25]

The initial slope of δ^s_{eL} as a function of Th concentration (Fig. 12) yields a value

$$\frac{\partial \delta^s_{eL}}{\partial c} = (5 \pm 2) \times 10^{+7} \text{ sec}^{-1}/\text{ppm Th in } LaAl_2 .$$

It should be mentioned that the same value (approximately) of $\partial \delta^s_{eL}/\partial c$ was observed from measurements on three different series of $Gd_yTh_xLa_{1-y-x}Al_2$ samples. This represents a remarkable success of the theory of Hasegawa.

In order to determine $\partial \delta^s_{eL}/\partial c$ for Gd in $LaAl_2$, we choose only those $Gd_xLa_{1-x}Al_2$ samples which exhibit small values of $\tau_{tr\,0}/\tau_{tr}$ ($\tau_{tr\,0}/\tau_{tr} = 0.5$ in Table I) to be sure that impurity contributions (other than Gd) to δ^s_{eL} are small. We find

$$\partial \delta^s_{eL}/\partial c = (1 \pm 0.6) \times 10^7 \text{ sec}^{-1}/\text{ppm Gd in } LaAl_2.$$

VI. SUMMARY

The use of (3) to obtain δ^s_{eL}, and the reduction of T_c to obtain δ^s_{ei} and then δ^s_{ie} from detailed balance, enables one to generate the complete magnetic-resonance parameters from superconductivity measurements, and vice versa. In terms of the magnetic-resonance experiments themselves, we are able to break the bottleneck in $LaAl_2$: Gd completely. Invoking the two-band (s and d) model, we are able to explain the apparent discrepancy between the g values for the concentrated compound and dilute alloy.

The close correlation between the parameters determining the superconducting and magnetic-resonance properties offers promise for the prediction of one, given the other. Thus, in materials where magnetic resonance is possible, it should be possible to predict those parameters which determine the thermal and magnetic superconducting properties.

*Supported in part by the National Science Foundation Grant No. GH-31973 and the U.S. Office of Naval Research Contract No. N00014-69-A-200-4032.

†On leave from the Institute of Physics, University of Silesia, Katwovice, Poland.

‡On leave from the Department of Physics, University of Buenos Aires, Argentina.

§ Supported by the U.S. Air Force Office of Scientific Research, Air Force System Command, under AFOSR Grant No. 71-2073.

[1]V. Jaccarino B. T. Matthias, M. Peter, H. Suhl, and J. H. Wernick, Phys. Rev. Lett. **5**, 251 (1960).

[2]D. Davidov and D. Shaltiel, Phys. Rev. **169**, 329 (1968).

[3]B. R. Coles, D. Griffith, R. J. Lowin, and R. H. Taylor, J. Phys. C **3**, 121 (1970).

[4]M. B. Maple, Phys. Lett. A **26**, 513 (1968).

[5]H. Hasegawa, Prog. Theor. Phys. **21**, 483 (1959).

[6]After correction because of possible dynamic effects.

[7]D. Davidov and D. Shaltiel, Phys. Rev. Lett. **21**, 1752 (1968).

[8]H. K. Schmidt, Z. Naturforsch. A **27**, 191 (1972).

[9]The resistivity ratio $\rho(300\,°K)/\rho(1.4\,°K)$ for samples prepared at the University of California, San Diego, is between 3 and 10. According to our estimate, the Landau-Ginzberg parameter κ, is large so that we are in the dirty limit.

[10]Takayoshi Mamiya, Toshio Aoi, Katsutoski Iwahashi, and Yashika Masuda, J. Phys. Soc. Jap. **31**, 485 (1971).

[11]A. A. Abrikosov and L. P. Gorkov, Zh. Eksp. Teor. Fiz. **39**, 1781 (1960) [Sov. Phys.-JETP 12, 1243 (1961)]; P. Fulde

and K. Maki, Phys. Rev. **141**, 275 (1966).

[12]E. D. Ramos and D. H. Sanchez, thesis (Rutgers University, 1971) (unpublished).

[13] R. D. Parks, in *Superconductivity*, edited by P. R. Wallace (Gordon and Breach, New York, 1969), Vol. II, p. 625.

[14]D. C. Hamilton and M. A. Jensen, [Phys. Rev. Lett. **11**, 205 (1963)] suggested that virtual scattering to a $4f$ level lying just above the Fermi level could serve as an explanation for the existence of superconductivity in La metal. Following this argument, R. E. Hungsberg and K. A. Geschneider [J. Phys. Chem. Solids **33**, 401 (1972)] suggested the $4f$ band lying close to the Fermi surface as an explanation of the larger γ for $LaAl_2$ as compared to YAl_2 and $LuAl_2$. We shall show that the EPR results are more consistent with an occupied d band.

[15]T. Moriya, J. Phys. Soc. Jap. **18**, 516 (1963); A. Narath and H. T. Weaver, Phys. Rev. **175**, 373 (1968); R. W. Shaw and W. W. Warren, Phys. Rev. B **3**, 1562 (1971).

[16] Y. Yafet and V. Jaccarino, Phys. Rev. **133**, 1630 (1964); A. Narath, in *Hyperfine Interactions*, edited by A. J. Freeman and R. B. Frankel (Academic, New York, 1967), p. 351.

[17]R. E. Hungsberg and K. A. Geschneider, Jr., J. Phys. Chem. Solids **33**, 401 (1972).

[18] W. L. McMillan, Phys. Rev. **167**, 331 (1967).

[19]M. B. Maple, Ph.D. thesis (University of California, San Diego, 1969) (unpublished).

[20]H. J. Van Daal and K. H. J. Buschow, Solid State Commun. **7**, 217 (1969).

[21]N. F. Mott, Proc. R. Soc. A **153**, 699 (1936).

[22]W. Schafer, H. K. Schmidt, B. Elschner, and K. H. J. Buschow, Phys. Lett. A**33**, 23 (1970).

[23]Detailed balanced condition in the presence of exchange enhancement of the conduction electron susceptibility has been derived microscopically by J. Zitkova (private communication). The conduction electron exchange spin flip rate δ_{ei} is exchange enhanced by the factor $K(\alpha)/(1-\alpha)$. The enhancement correction for the conduction electron spin-orbit spin-flip rate [W. F. Brinkman and S. Engelsberg, Phys. Rev. Lett. **21**, 1187 (1968)] is simply $1-\alpha$. The difference results from the absence of spin-orbit vertex renormalization in the latter by virtue of vanishing angular averages.

[24] Y. Yafet, J. Appl. Phys. **39**, 853 (1968).

[25] K. H. Bennemann and J. W. Garland, Intern. J. Magnetism **1**, 97 (1971).